


Article

Super Capacitor Energy Storage Based MMC for Energy Harvesting in Mine Hoist Application

Xiaofeng Yang ^{1,*} , Piao Wen ¹, Yao Xue ¹, Trillion Q. Zheng ¹ and Youyun Wang ²

¹ School of Electrical Engineering, Beijing Jiaotong University, Beijing 100044, China;

17121507@bjtu.edu.cn (P.W.); 16117392@bjtu.edu.cn (Y.X.); tqzheng@bjtu.edu.cn (T.Q.Z.)

² Tianshui Electric Drive Research Institute Co. LTD, Tianshui 741020, China; wyy@vip.163.com

* Correspondence: xfyang@bjtu.edu.cn; Tel.: +86-10-5168-7064

Received: 23 August 2017; Accepted: 13 September 2017; Published: 17 September 2017

Abstract: This paper proposes a super capacitor energy storage-based modular multilevel converter (SCES-MMC) for mine hoist application. Different from the conventional MMCs, the sub-modules employ distributed super capacitor banks, which are designed to absorb the regenerative energy of mine hoist and released in the traction condition, so as to improve energy utilization efficiency. The key control technologies are introduced in detail, followed by analysis of the configuration and operation principles. The feasibility of the proposed SCES-MMC topology and the control theory are also verified. Simulation results show that SCES-MMC can adapt to the variable frequency speed regulation of the motor drive, which shows good application prospects in the future for medium- and high-voltage mine hoist systems.

Keywords: super capacitor energy storage (SCES); modular multilevel converter (MMC); mine hoist; state of charge; regenerative energy; energy harvesting

1. Introduction

The mine hoist conveyor is typically one of the largest consumers of electric power, besides of the excavator systems, of all equipment in the mining industry. As the only inoue-to-downhole access, the output performance of mine hoist electric transmission systems may not only play key roles in economical mine production, but may also affect equipment and personal safety [1,2]. In view of the large power rating requirements for mine hoist electric transmission systems, medium-voltage source converters (VSC) have increasingly gained importance due to their high power density, excellent efficiency, and high reliability [3–5]. For the last two decades, three-level neutral-point-clamped (NPC) VSCs have been the standard solution in the medium-voltage range for industrial applications [6,7]. Since the regenerative energy in an electric mine hoister and excavator may be as high as 60 percent of the motoring power [8,9], active front-end rectifiers (AFE) are usually adopted to feed the regenerative energy back into the power distribution grid in order for it not to be wasted. However, the practical constraints in the controller bandwidth may place restrictions on the system's regenerative power handling. Therefore, protective circuits, such as DC choppers and crowbars, are usually added to the system for suppressing the DC bus over-voltage during regeneration [10].

Compared with NPC-VSC, modular multilevel converter (MMC) provides advantages such as high modularity, lower switching efficiency, high efficiency, better output voltage performance, etc. Thus, in addition to its successful commercial implementation in high voltage direct current (HVDC) transmission projects [11–13], it also shows good application prospects in fields such as power quality control [14,15]. However, AC drive-based MMCs are only suitable for industrial fans, pumps and other applications of small speed range close to the rated value. In order to solve the low-frequency torque ripple issues of conventional MMC motor drive systems, many scholars have

carried out extensive research and proposed control strategies for common mode voltage/current multi-component injection and pulse optimization [16–19]. However, the above method does not fundamentally eliminate the limitations of MMC variable frequency-speed regulation control. On the other hand, domestic mine accidents have been frequent in recent years. If the high-voltage converter could continue to operate for a short time under outage conditions, the reliability of the mine hoist equipment would be significantly improved. In addition, when the mine hoist is braking, the electric transmission system will be in the generation condition, and the regenerating energy will charge the DC bus capacitor. An energy storage-enabled MMC seems an ideal solution for the abovementioned issues, since the super capacitors show better power density and a longer service life compared to traditional batteries. Thus, the super capacitor energy storage based MMC (SCES-MMC) is more suitable for mine hoist application. However, published technical papers focus mainly on battery energy storage system (BESS)-based MMCs [20,21]. In view of the above issues, this paper adopts the SCES-MMC for energy-harvesting applications. The super capacitor banks within the SCES-MMC operates as a power source to ensure the mine hoist keeps working for a short time when power failures occur unexpectedly. As a result, the safety of the mine hoist equipment can be significantly improved to avoid mine accidents. In addition, when the mine hoist is braking, the regenerative energy is quickly transferred to the SCES to avoid DC bus overvoltage.

This paper is organized as follows. Section 2 presents the structural characteristics and operation principles of SCES-MMC topology. In Section 3, the system control strategies including motor frequency controls and state of charge (SOC) balancing controls are explored in detail. To validate the feasibilities and effectiveness of the proposed topology and theory, extensive simulation results are demonstrated in Section 4. Finally, Section 5 reports the main conclusions.

2. Topology and Operation Principles

2.1. Topology Analysis

A typical topology for three-phase SCES-MMC is shown in Figure 1, where L_s is the output equivalent AC inductance, o is the neutral point of reference potential between the positive P and negative N of the DC bus. The SCES-MMC is three-phase balanced, and its phase-leg consists of $2n$ sub-modules SM_{jk} (phase $j = a, b, c$, SMs number $k = 1, 2, \dots, 2n$) and leg inductance L_a . Figure 1b shows the basic building blocks-SCES-SM, which consists of two IGBTs (T_1, T_2), two anti-parallel diodes (D_1, D_2), a capacitor C_{SM} , a super capacitor bank interface circuit.

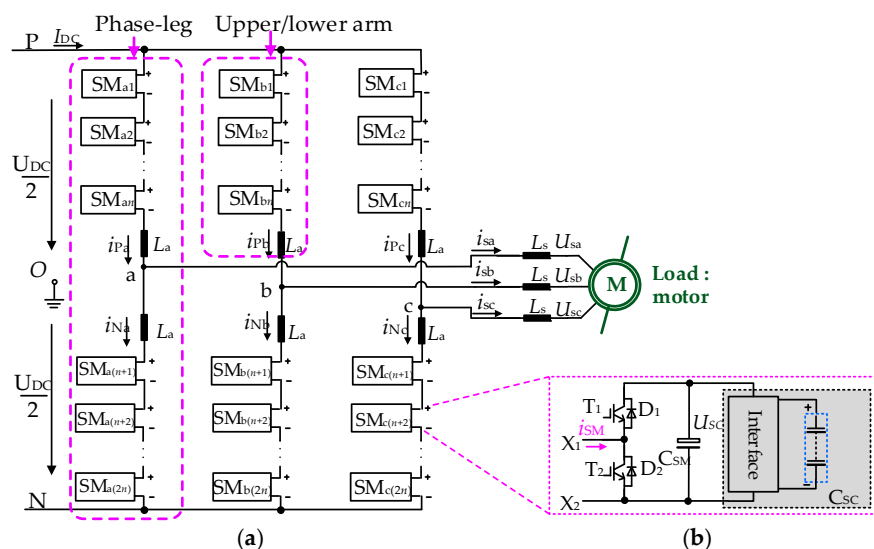


Figure 1. Configuration of three-phase SCES-MMC and its sub-module: (a) Three-phase SCES-MMC topology; (b) SCES-SM.

Figure 2 demonstrates three widely-applied topologies for SCES-SM interface circuits: direct connection, bidirectional buck/boost converter and dual active bridge converter. The main difference between the latter two is the isolating transformer. To simplify the analysis, Figure 2a is selected as the SCES-SM interface circuit, but this does not affect the correctness of the theory. Additionally, the distributed super capacitors C_{SC} results in an SCES-MMC with a highly modular structure and redundant capability, which further improves the reliability of the SCES-MMC for mine hoist applications. What is more, the circulating energy of SCES-MMC is exchanged between phase-legs through the common DC bus. Therefore, the SCES-SMs' state of charge (SOC) may also be applied for system controls.

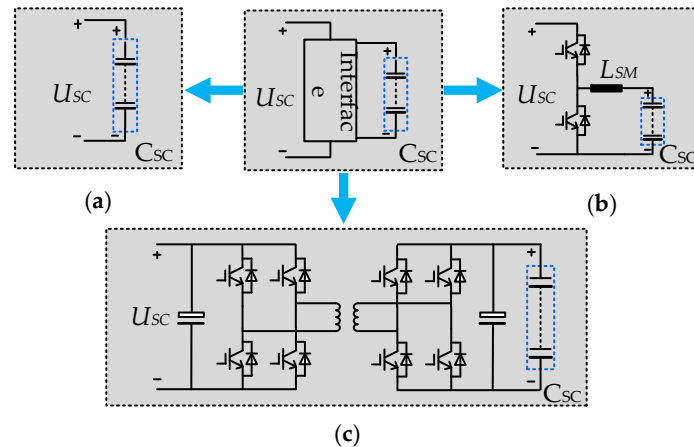


Figure 2. Topology of SCES-SM interface circuit: (a) Direct connection (b) Bidirectional buck/boost converter (c) Dual active bridge converter.

2.2. Operation Principles of SCES-MMC

The switching states of the SCES-SM are shown in Table 1, and the output voltage of SCES-SM is switched between zero and U_{SC} by controlling T_1 and T_2 , where U_{SC} is the DC voltage of the SCES-SM. At the same time, SOC control of the corresponding super capacitor banks (SCBs) may also be implemented in this process.

Table 1. Switching states of SCES-SM.

Mode	T_1/D_1	T_2/D_2	i_{SM}	Output Voltage	SOC
Charging	0/1	0/0	>0	U_{SC}	increasing
Discharging	1/0	0/0	<0	U_{SC}	decreasing
Bypass	0	1	>0	0	maintaining
Bypass	0	1	<0	0	maintaining

According to the reference direction shown in Figure 1, AC current of phase- j during normal operation is expressed as

$$i_{Pj} = \frac{1}{3}I_{DC} + \frac{1}{2}i_{sj} + i_{Zj} \tag{1}$$

$$i_{Nj} = \frac{1}{3}I_{DC} - \frac{1}{2}i_{sj} + i_{Zj} \tag{2}$$

$$i_{sj} = i_{Pj} - i_{Nj} \tag{3}$$

$$i_{Cj} = \frac{1}{3}I_{DC} + i_{Zj} \tag{4}$$

where i_{pj} and i_{Nj} are the upper and lower arm currents, respectively; I_{DC} is the DC bus current. The arm current flows through both the upper and lower legs consist of half of the AC output current i_{sj} and the common-mode current i_{Cj} , which consists of the DC component $I_{DC}/3$ and the circulating component i_{Zj} . The former refers to the active power for charging and discharging the SM capacitors, while the latter indicates the reactive power causing the SM capacitor voltage ripples. Similarly, the resulting AC and DC voltages are determined by

$$u_{pj} = \frac{U_{DC}}{2} - u_j - L_a \frac{di_{pj}}{dt} - R_a i_{pj} \tag{5}$$

$$u_{Nj} = \frac{U_{DC}}{2} + u_j - L_a \frac{di_{Nj}}{dt} - R_a i_{Nj} \tag{6}$$

$$u_j = \frac{u_{Nj} - u_{pj}}{2} - \frac{L_a}{2} \frac{di_j}{dt} - \frac{R_a}{2} i_j \tag{7}$$

$$U_{DC} = u_{pj} + u_{Nj} + 2L_a \frac{di_{Cj}}{dt} + 2R_a i_{Cj} \tag{8}$$

where u_j is the AC output phase voltage, U_{DC} is the rated DC bus voltage, R_a is the equivalent series arm resistor, and u_{pj} and u_{Nj} denote the upper and lower arm voltages, respectively.

2.3. Power Flow Analysis

Figure 3 illustrates the power flow modes, where P_{SCES} refers to the power absorbed/released by SCES, the load side power P_{load} is represented by P_{trac} when under traction conditions, or by P_{reg} when under regeneration conditions. The fundamental power exchange relation is as follows

$$P_{Load} = P_{dc} + P_{SCES} \tag{9}$$

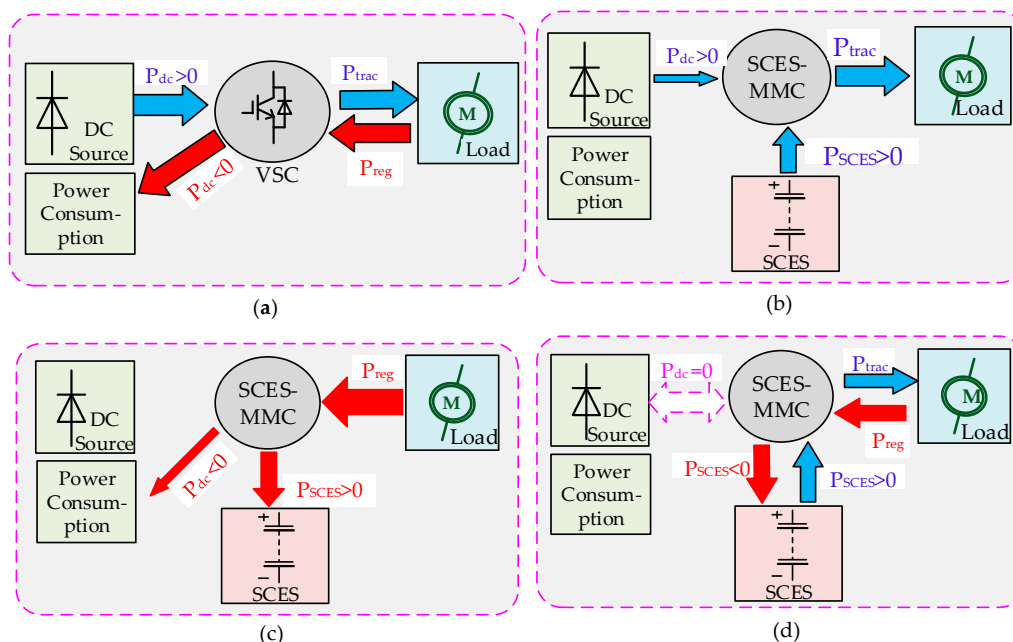


Figure 3. Illustration of power flow: (a) Conventional VSC without SCES; (b) Traction (discharging) condition; (c) Regeneration (charging) condition; (d) Fault operation mode.

With regard to bidirectional power flow characteristics, SCES-SM charging/discharging is realized through different operation modes. The two basic operation modes in SCES-MMC are defined as follows.

1. Normal operation mode: $|P_{Load}| > |P_{dc}|$
 Mode (a): $P_{Load} = P_{dc}, P_{SCES} = 0$;
 Mode (b): $P_{dc} > 0, P_{SCES} > 0$ (discharging), $P_{trac} > 0$ (traction condition);
 Mode (c): $P_{dc} < 0, P_{SCES} < 0$ (charging), $P_{reg} > 0$ (regeneration condition);
2. Fault operation mode: $P_{dc} = 0$
 Mode (d): $P_{Load} = P_{SCES}$.

In mode (a), SCES does not participate in the work. As a result, the operation principles of SCES-MMC are similar to the conventional MMCs. Load side power is fed exclusively from the DC bus of the SCES-MMC. Notably, when the mine hoist motor is braking, the regenerative energy may be consumed on the DC bus due to the uncontrolled rectifier, as shown in Figure 3a.

In mode (b), the load side motor is under traction conditions, and the SCES functions as the DC source; thus, SCBs discharge to provide part of the AC load power, as shown in Figure 3b.

In mode (c), the load side motor is under regenerative conditions, and the SCES absorbs part of the regenerative power from the mine hoist motor. However, extra regenerative power is still consumed on the DC bus.

In contrast to conventional MMCs, when power outage faults occur, SCES will play the role of sole DC source, and feed the AC side load under similar control strategies as those shown in Figure 3d; thus, the mine hoist motor system is capable of continuing to work for a short time. This is a major advantage of SCES-MMC in terms of enhancing system reliability.

3. System Control Strategies

The SCES-MMC operates differently from regular MMCs. Since the SCBs within each SCES-SM are able to act as the DC source for supplying the AC load, the power will be delivered not only from the DC bus but also the SCES. Therefore, the SCES-MMC control strategy, when applied to the mine hoist motor drive system, includes two main parts, namely, motor variable frequency speed regulation (VFSR) control and SOC control.

3.1. Variable Frequency Speed Control

The typical operating states of the mine hoist include acceleration, uniform speed, and deceleration; thus, speed regulation is one of the main control targets. Based on the active flux observer (AFO)-based variable frequency speed regulation control proposed in [22,23], the SCES-MMC VFSR control strategy proposed in this paper is shown in Figure 4, where ω^* and ω are the reference mine hoist rotor speed and the observed rotor speed obtained by the active flux observer (AFO) proposed in [22,23], respectively. The reference current i_q^*, i_d^* is calculated according to the mathematical model of synchronous motors, as proposed in [22]. Proportional integral regulator PI refers to the current loop controller. Consequently, the upper- and lower-arm voltages u_{pj}^* and u_{Nj}^* are calculated based on Equations (5) and (6).

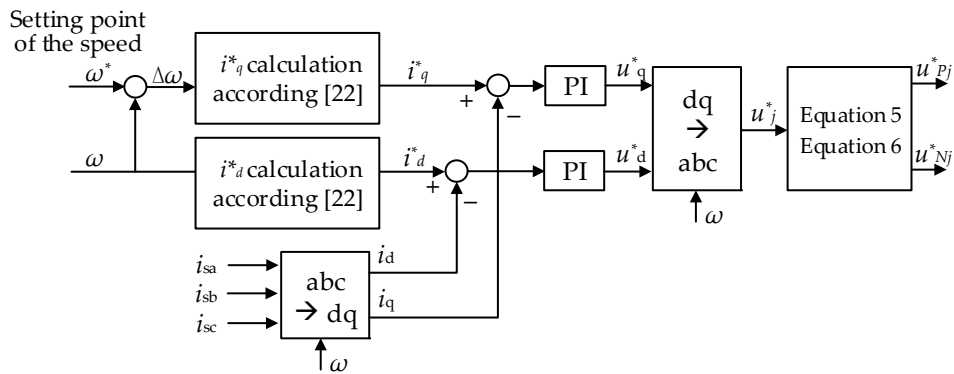


Figure 4. Block diagram of variable frequency speed control.

3.2. SOC Control

SOC control is one of the main differences from conventional MMCs. It is essential to control the circulating current of SCES-MMC to maximize the efficiency of the SOC controls. According to the configuration features, The SOC control structure of SCES-MMC generally includes SOC control of upper/lower arm sub-modules and SOC balancing control of phase-legs, as shown in Figure 5, where K_2 to K_5 refer to closed-loop controllers such as PI controllers.

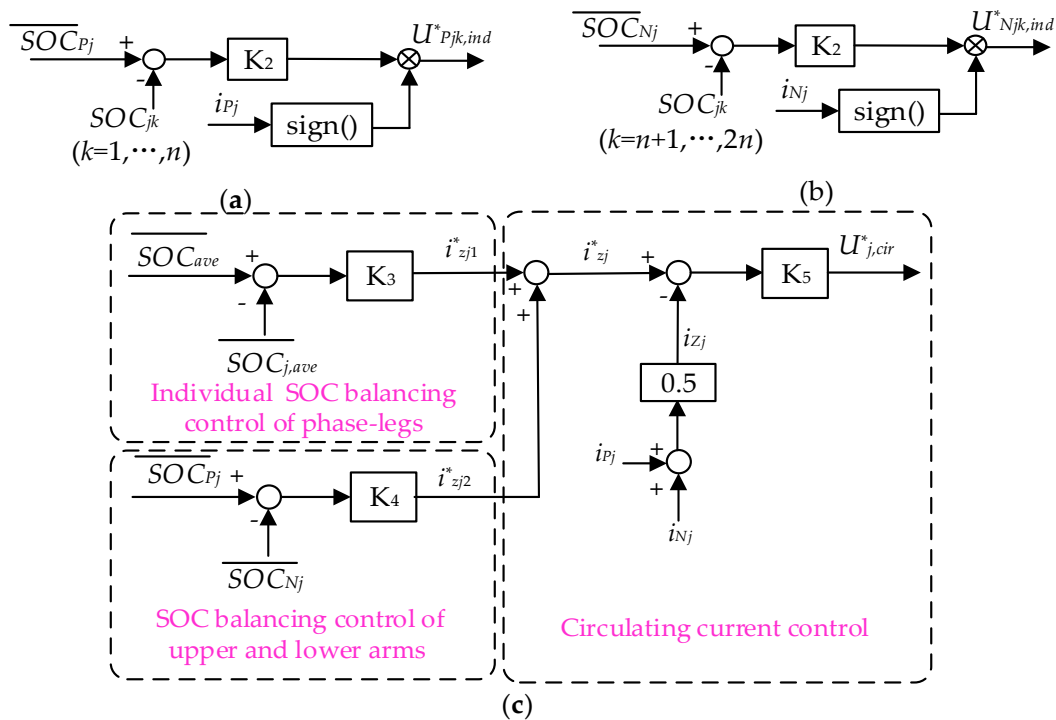


Figure 5. Block diagram of SOC control: (a) Individual SOC control (upper arm); (b) Individual SOC control (lower arm); (c) SOC balancing control.

Figure 5a,b shows the block diagram of individual SOC balancing controls, so as to make the SCES-SM SCBs SOC on the same leg equal to its corresponding average arm SOC (\overline{SOC}_{Pj} , \overline{SOC}_{Nj}). sign() denotes the signum function, and the average arm SOC \overline{SOC}_{Pj} , \overline{SOC}_{Nj} are expressed as follows:

$$\overline{SOC}_{Pj} = \frac{1}{n} \sum_{k=1}^n SOC_{jk} \tag{10}$$

$$\overline{SOC}_{Nj} = \frac{1}{n} \sum_{k=n+1}^{2n} SOC_{jk} \quad (11)$$

The arm SOC balancing control aims to eliminate the deviation between the average arm SOC. Similarly, the SOC balancing control of the phase-legs aims to eliminate the deviation between the average SOC ($\overline{SOC}_{j,ave}$) of each phase and the three-phase average SOC (\overline{SOC}_{ave}). Therefore, $\overline{SOC}_{j,ave}$ and \overline{SOC}_{ave} are given by:

$$\overline{SOC}_{j,ave} = \frac{1}{2n} \sum_{k=1}^{2n} SOC_{jk} \quad (12)$$

$$\overline{SOC}_{ave} = \frac{1}{3} \sum_{j=a}^c \overline{SOC}_{j,ave} \quad (13)$$

The above SOC control is implemented by the control of the circulating current, and the reference circulating current i_{Zj}^* is calculated from the outputs of the above two SOC balancing control i_{Zj1}^* and i_{Zj2}^* , as follows

$$i_{Zj}^* = i_{Zj1}^* + i_{Zj2}^* \quad (14)$$

The controller of the circulating current inner loop aims to make the actual circulating current i_{zj} equal to the reference current i_{Zj}^* , and then to realize the SOC balancing control, with the reference voltage $U_{j,cir}^*$ being the output of the controller.

In summary, system control structures for the SCES-MMC are shown as Figure 6, where the reference voltage of the phase arm is calculated as follows:

$$U_{Pjk}^* = \frac{u_{Pj}^*}{n} + U_{Pjk,ind}^* + U_{j,cir}^* + \frac{U_{DC}^*}{n} \quad (15)$$

$$U_{Njk}^* = \frac{u_{Nj}^*}{n} + U_{Njk,ind}^* + U_{j,cir}^* + \frac{U_{DC}^*}{n} \quad (16)$$

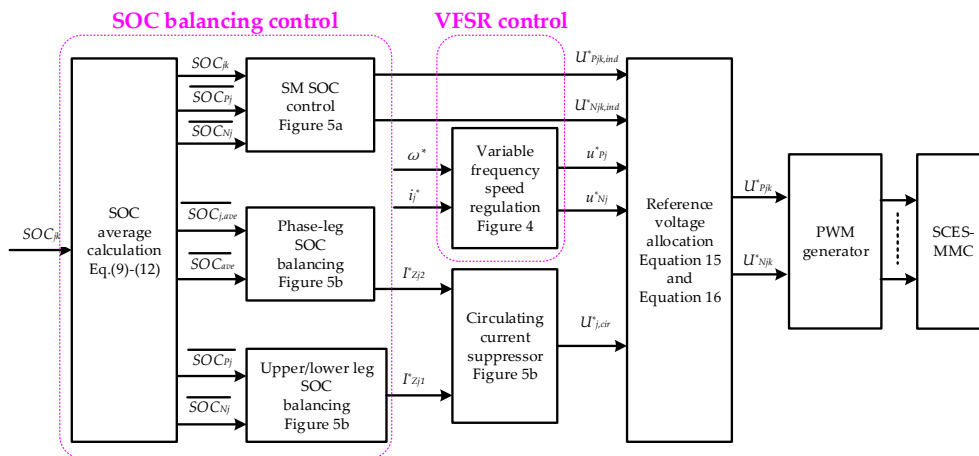


Figure 6. Overview of system control structures for SCES-MMC.

4. Verifications of SCES-MMC

To verify the feasibility of the proposed SCES-MMC mine hoist system and control strategies, a simulation model of a nine-level SCES-MMC was created, as shown in Figure 7. The multi-pulse rectifier and chopper cell are employed to supply the constant DC bus voltage U_{DC} . The simulation model parameters of SCES-MMC are listed in Table 2, and the initial SOC value of the SCBs is 100%. The super capacitor parameter design and selection method are similar to [24], and the modulation method adopted in this simulation is carrier phase-shifted sinusoidal pulse-width-modulation,

combined with the third harmonic injection method of [25]. In addition, assuming that the synchronous motor reaches the rated speed at 0.6 s and starts decelerating at 0.9 s, the SCES-MMC output performance is shown in Figure 8.

Figure 8a,b shows that the frequency of the voltage and the current will gradually rise to its rated value under variable frequency speed regulation control. The SCES-MMC comes to its steady state at 0.6 s, and then gradually decays when the system enters the deceleration condition at 0.9 s. From the speed characteristics of the synchronous motor shown in Figure 8c, it can be seen that, before 0.6 s, the SCBs begin to release energy when the motor speed is rising and the system SOC is decreasing, as shown in Figure 8d. Then, the motor speed starts to drop when the synchronous motor brakes at 0.9 s, and the regenerative power in this process will also help charge the SCB of each SCES-SM, hence its SOC will rise.

Table 2. Simulation parameters of SCES-MMC.

System Parameters	Value
AC line-to-line voltage	1.45 kV
DC link voltage	3.6 kV
Rated power	5.3 MW
Leg inductance	5.0 mH
SM capacitor voltage	0.45 kV
Super capacitor capacitance	20 F
Rated speed	52 rpm

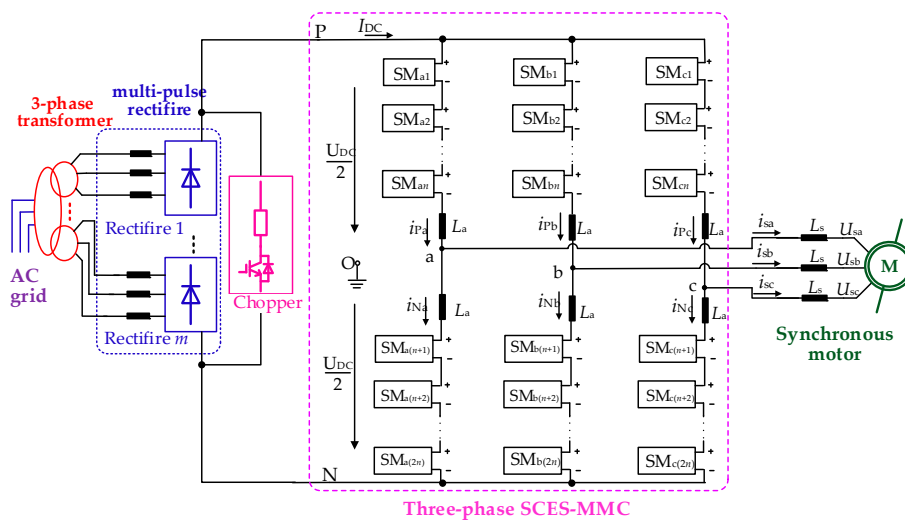


Figure 7. Configuration of SCES-MMC simulation model.

Due to the high capacitance of the SCBs, even if a large amount of energy is released/absorbed, there is no significant fluctuation in the sub-module capacitor voltage U_{SM} , as shown in Figure 8e,f.

Figure 9 illustrates the power distribution laws of the proposed SCES-MMC. From the above-mentioned analysis, it can be concluded that the SCBs in the SCES-MMC will be discharged to provide about 69% of the AC load power requirement. Thus, less DC power is required compared to those without super capacitor banks. Since SCES is involved in absorbing part of the regenerative power from the mine hoist motor, under regeneration conditions, the power dissipated in the SCES-MMC is also less than for conventional MMCs. This makes it possible to minimize the capacity requirements of the AC grid and energy loss of the mine hoist system.

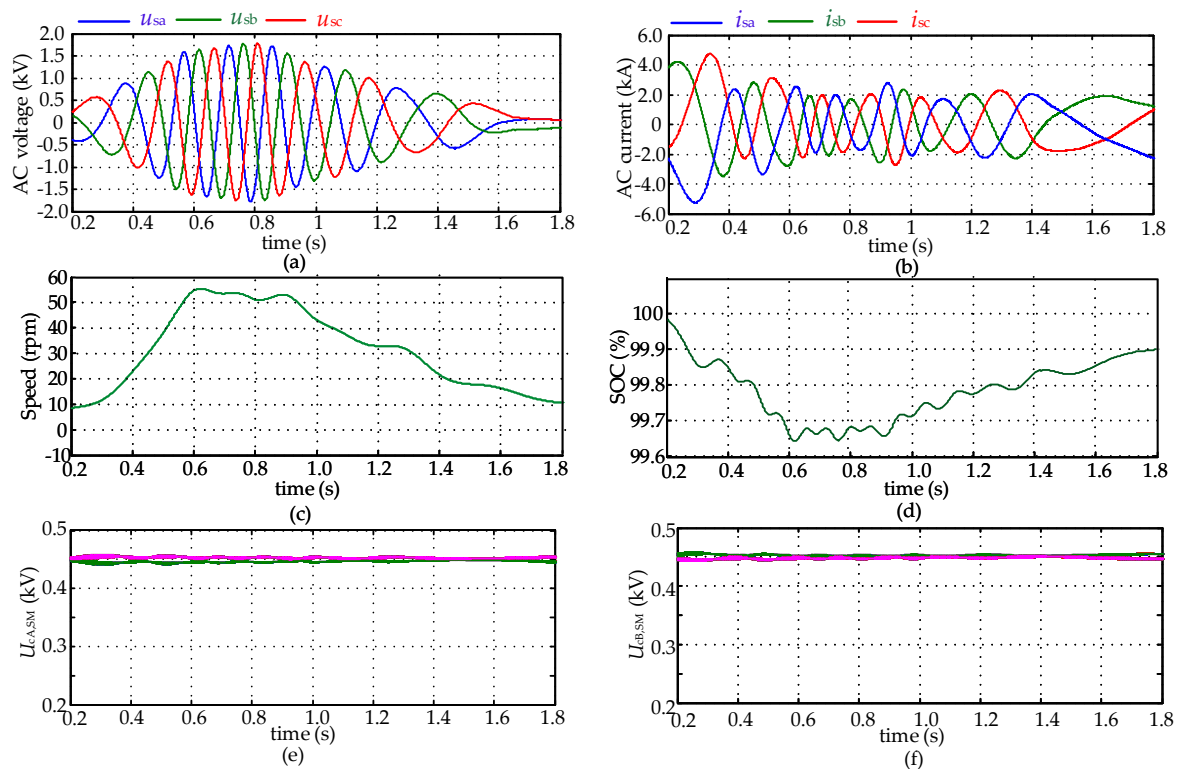


Figure 8. Output performance of SCES-MMC: (a) AC output voltage; (b) AC output current; (c) Motor speed; (d) Average SOC of SCBs; (e) Voltage of the SCBs—phase a; (f) Voltage of the SCBs—phase b.

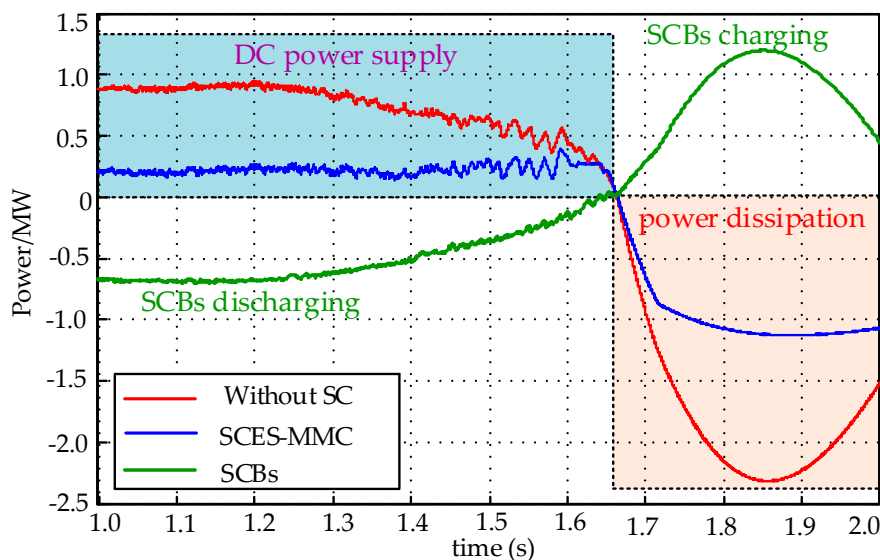


Figure 9. Power distributions.

5. Conclusions

A super capacitor energy storage-based modular multilevel converter (SCES-MMC) topology for mine hoist applications has been investigated in this paper. In contrast to conventional MMCs, the sub-modules employ distributed SCBs, which are designed to absorb the regenerative energy of the mine hoist, and release it under traction conditions. Due to the high power density of the super capacitor, the sub-modules' capacitor voltage will not significantly fluctuate. The configuration and operation principles, together with control technologies were studied in detail. Moreover, the

feasibility of the proposed SCES-MMC topology and the control theory were also verified. Simulation results show that SCES-MMC makes reasonable use of the energy of the system through the distributed SCBs, improving the energy utilization efficiency, and shows good application prospects in future medium-/high-voltage mine hoist systems.

Acknowledgments: The authors gratefully acknowledge technical support from the National Key Research and Development Program of China (Award Number: 2016YFE0131700) and the State Key Laboratory of Large Electric Drive System and Equipment Technology (Award Number: SKLLDJ042016005).

Author Contributions: Xiaofeng Yang contributed to the concept, undertook significant theory analysis, and wrote the paper. Piao Wen and Yao Xue helped perform the simulation with constructive discussions, Trillion Q. Zheng supplied guidance, and Youyun Wang provided the field testing parameters and edited the manuscript. All authors read and approved the manuscript.

Conflicts of Interest: The authors declare no conflicts of interest.

Abbreviations

The following abbreviations are used in this manuscript:

AC	alternating current
DC	direct current
HVDC	high voltage direct current
VSC	voltage source converter
NPC	neutral-point-clamped
AFE	active front end
SCES	super capacitor energy storage
MMC	modular multilevel converter
SM	sub-module
SCB	super capacitor bank
SOC	state of charge
IGBT	insulated gate bipolar transistor
VFSR	variable frequency speed regulation

References

- Chen, H. Research and Application Based on Full Digital DC Speed Adjusting Device in Mine Hoist Automation System. In Proceedings of the International Symposium on Intelligence Information Processing and Trusted Computing, Huanggang, China, 28–29 October 2010; pp. 524–527.
- Ferreira, V.N.; Mendonça, G.A.; Rocha, A.V.; Resende, R.S.; Cardoso Filho, B.J. Medium voltage IGBT-based converters in mine hoist systems. In Proceedings of the IEEE Industry Applications Society Annual Meeting, Portland, OR, USA, 2–6 October 2016; pp. 1–8.
- Abu-Rub, H.; Holtz, J.; Rodriguez, J.; Ge, B. Medium-Voltage Multilevel Converters—State of the Art, Challenges, and Requirements in Industrial Applications. *IEEE Trans. Ind. Electron.* **2010**, *57*, 2581–2596. [[CrossRef](#)]
- Kouro, S.; Malinowski, M.; Gopakumar, K.; Pou, J.; Franquelo, L.G.; Bin, W.; Rodriguez, J.; Perez, M.A.; Leon, J.I. Recent Advances and Industrial Applications of Multilevel Converters. *IEEE Trans. Ind. Electron.* **2010**, *57*, 2553–2580. [[CrossRef](#)]
- Yang, X.; Li, J.; Wang, X.; Fan, W.; Zheng, T.Q. Circulating Current Model of Modular Multilevel Converter. In Proceedings of the Asia-Pacific Power and Energy Engineering Conference (APPEEC), Wuhan, China, 25–28 March 2011; pp. 1–6.
- Krug, D.; Malinowski, M.; Bernet, S. Design and comparison of medium voltage multi-level converters for industry applications. In Proceedings of the 39th IEEE Industry Applications Conference (IAS), Seattle, WA, USA, 3–7 October 2004; pp. 781–790.
- Asea Brown Boveri. *ACS 6000 Medium Voltage AC Drives—Commissioning Manual*; ABB Switzerland Ltd.: Zurich, Switzerland, 2004.

8. Abdel-baqi, O.; Nasiri, A.; Miller, P. Dynamic Performance Improvement and Peak Power Limiting Using Ultracapacitor Storage System for Hydraulic Mining Shovels. *IEEE Trans. Ind. Electron.* **2015**, *62*, 3173–3181. [[CrossRef](#)]
9. Parkhideh, B.; Mirzaee, H.; Bhattacharya, S. Supplementary Energy Storage and Hybrid Front-End Converters for High-Power Mobile Mining Equipment. *IEEE Trans. Ind. Appl.* **2013**, *49*, 1863–1872. [[CrossRef](#)]
10. Parkhideh, B.; Bhattacharya, S.; Mazumdar, J.; Koellner, W. Utilization of Supplementary Energy Storage Systems in High Power Mining Converters. In Proceedings of the 2008 IEEE Industry Applications Society Annual Meeting, Edmonton, AB, Canada, 5–9 October 2008; pp. 1–7.
11. Dorn, J.; Huang, H.; Retzmann, D. Novel Voltage-Sourced Converters for HVDC and FACTS Applications. In Proceedings of the CIGRE Symposium, Osaka, Japan, 1–4 November 2007; pp. 314–321.
12. Yang, X.; Xue, Y.; Chen, B.; Lin, Z.; Mu, Y.; Zheng, T.Q.; Igarshi, S. Reverse blocking sub-module based modular multilevel converter with DC fault ride-through capability. In Proceedings of the IEEE Energy Conversion Congress and Exposition (ECCE), Milwaukee, WI, USA, 18–22 September 2016; pp. 1–7.
13. Yang, X.; Xue, Y.; Chen, B.; Lin, Z.; Zheng, T.Q.; Li, Y. Novel modular multilevel converter against DC faults for HVDC applications. *CSEE J. Power Energy Syst.* **2017**, *3*, 140–149.
14. Ma, F.; Xu, Q.; He, Z.; Tu, C.; Shuai, Z.; Luo, A.; Li, Y. A Railway Traction Power Conditioner Using Modular Multilevel Converter and Its Control Strategy for High-Speed Railway System. *IEEE Trans. Transp. Electr.* **2016**, *2*, 96–109. [[CrossRef](#)]
15. Yang, X.; Zheng, T.Q.; Lin, Z.; Tao, X.; You, X. Power Quality Controller Based on Hybrid Modular Multilevel Converter. In Proceedings of the the 21st IEEE International Symposium on Industrial Electronics (ISIE), Hangzhou, China, 28–30 May 2012; pp. 1997–2002.
16. Hagiwara, M.; Akagi, H.; Nishimura, K. A Medium-Voltage Motor Drive with a Modular Multilevel PWM Inverter. *IEEE Trans. Ind. Electron.* **2010**, *25*, 1786–1799. [[CrossRef](#)]
17. Li, B.; Zhou, S.; Xu, D.; Yang, R.; Xu, D.; Buccella, C.; Cecati, C. An Improved Circulating Current Injection Method for Modular Multilevel Converters in Variable-Speed Drives. *IEEE Trans. Ind. Electron.* **2016**, *63*, 7215–7225. [[CrossRef](#)]
18. Antonopoulos, A.; Angquist, L.; Harnefors, L.; Nee, H. Optimal Selection of the Average Capacitor Voltage for Variable-Speed Drives With Modular Multilevel Converters. *IEEE Trans. Ind. Electron.* **2015**, *30*, 227–234. [[CrossRef](#)]
19. Kolb, J.; Kammerer, F.; Gommeringer, M.; Braun, M. Cascaded Control System of the Modular Multilevel Converter for Feeding Variable-Speed Drives. *IEEE Trans. Power Electron.* **2015**, *30*, 349–357. [[CrossRef](#)]
20. Vasiladiotis, M.; Rufer, A. A Modular Multiport Power Electronic Transformer with Integrated Split Battery Energy Storage for Versatile Ultrafast EV Charging Stations. *IEEE Trans. Ind. Electron.* **2015**, *62*, 3213–3222.
21. Quraan, M.; Yeo, T.; Tricoli, P. Design and Control of Modular Multilevel Converters for Battery Electric Vehicles. *IEEE Trans. Power Electron.* **2016**, *31*, 507–517. [[CrossRef](#)]
22. Agarlita, S.; Coman, C.; Andreescu, G.; Boldea, I. Stable V/f control system with controlled power factor angle for permanent magnet synchronous motor drives. *IET Electron. Power Appl.* **2013**, *7*, 278–286. [[CrossRef](#)]
23. Boldea, I.; Paicu, M.C.; Andreescu, G. Active Flux Concept for Motion-Sensorless Unified AC Drives. *IEEE Trans. Power Electron.* **2008**, *23*, 2612–2618. [[CrossRef](#)]
24. Sau, S.; Fernandes, B.G. Analysis and reduction of capacitor ripple current in modular multilevel converter for variable speed drives. In Proceedings of the European Conference on Power Electronics and Applications (EPE'16 ECCE Europe), Karlsruhe, Germany, 5–9 September 2016; pp. 1–10.
25. Li, R.; Fletcher, J.E.; Williams, B.W. Influence of third harmonic injection on modular multilevel converter-based high-voltage direct current transmission systems. *IET Gener. Transm. Distrib.* **2016**, *10*, 2764–2770. [[CrossRef](#)]

